Journal of Inorganic and Organometallic Polymers and Materials
https://doi.org/10.1007/s10904-024-03235-9

RESEARCH

Endophytic Fungus *Colletotrichum siamense* Derived Silver Nanoparticles: Biomimetic Synthesis, Process Optimization and Their Biomedical Applications

Frazer Andrade[1] · Christopher Jenipher[2] · Nilambari Gurav[3] · Sameer Nadaf[4] · Mohd Shahnawaz Khan[5] · Mohan Kalaskar[6] · Somnath Bhinge[7] · Ritesh Bhole[8] · Muniappan Ayyanar[2] · Shailendra Gurav[1]

Received: 22 May 2024 / Accepted: 22 June 2024

Abstract

The present study validates the biomimetic synthesis of silver nanoparticles using an endophytic fungus, *Colletotrichum siamense* Prihast (*Colleto*-AgNPs) derived from *Annona muricata* leaves. The study also investigates the impact of various process variables, including reductant concentration, the ratio of $AgNO_3$ to reductant concentration, reaction time, and reaction pH, on achieving optimal efficiency using a factorial design approach (Box Behnken Design experiment). The presence of nanoparticles was verified by observing absorption peaks in the 400–500 nm range. The TEM and SEM-EDX analysis reveals the presence of spherical form nanoparticles. In XRD, a strong peak at 38.10º diffraction indicated that the formed silver crystal was perpendicular to the plane. The average particle size was recorded as 98.48 nm, and the polydispersity index was 0.198 with a zeta potential of -4.92 mV. The toxicity of synthesized *Colleto*-AgNPs was assessed using brine shrimp lethality bioassay (LC_{50} of 312.51 ± 32.54 µg/mL). The minimum inhibitory concentration (MIC) of *Colleto*-AgNPs was determined and reported to be highly effective in suppressing *Escherichia coli*, *Listeria monocytogenes*, *Staphylococcus aureus*, and *Salmonella typhimurium*. In the agar well diffusion method, *Colleto*-AgNPs showed strong inhibitory effect against *L. monocytogenes* (23.98 mm), *S. aureus* (22.9 mm), *E. coli* (20.23 mm), and *S. typhimurium* (17.76 mm) at lower concentrations. *Colleto*-AgNPs exhibited a significant inhibitory effect against the α-amylase (IC_{50} of 30.57 ± 0.17 µg/mL) and α-glucosidase (IC_{50} of 32.30 ± 1.23 µg/mL) enzymes and DPPH radical (IC_{50} of 26.98 ± 0.30 µg/mL). By conceding this, further investigation can be conducted on *Colleto*-AgNPs for pre-clinical trials, which would be advantageous in developing innovative medications without any negative side effects for the betterment of humanity.

Keywords *Annona muricata* · Antibacterial · Endophytes · Process variables · Silver nanoparticles

Frazer Andrade and Christopher Jenipher contributed equally to this work.

✉ Muniappan Ayyanar
asmayyanar@yahoo.com

✉ Shailendra Gurav
shailendra.gurav@nic.in

[1] Department of Pharmacognosy, Goa College of Pharmacy, Goa University, Goa 403 001, India

[2] Department of Botany, A.V.V.M. Sri Pushpam College (Autonomous), Poondi (Affiliated to Bharathidasan University), Thanjavur 613 503, India

[3] PES's Rajaram and Tarabai Bandekar College of Pharmacy, Goa University, Ponda, Goa 403401, India

[4] Bharati Vidyapeeth College of Pharmacy, Palus, Maharashtra, India

[5] Department of Biochemistry, College of Science, King Saud University, Riyadh, Saudi Arabia

[6] R.C. Patel Institute of Pharmaceutical Education and Research, Shirpur, India

[7] Department of Pharmaceutical Chemistry, Rajarambapu College of Pharmacy, Shivaji University, Kasegaon, Kolhapur, Maharashtra 415404, India

[8] Dr. D. Y. Patil Institute of Pharmaceutical Sciences and Research, Pimpri, Pune 411018, India

Published online: 27 July 2024

1 Introduction

Nanoscale materials with exceptional properties have catapulted nanotechnology into the limelight, with applications spanning electronics, medicine, textiles, and environmental protection. Because of the high surface-to-volume ratios and capacity to range in at least one dimension between 1 and 100 nm, nanoparticles are incredibly powerful materials. The particle size of nanoparticles is influenced not only by their surface area to volume ratio but also by their physical, biological, and chemical properties, which differ from those of their conventional substance [1]. Researchers have examined the antimicrobial properties of several nanomaterials, including copper, zinc, gold, and silver, against various microbiological infections. Researchers have found that silver nanoparticles have many valuable characteristics, including their potent antibacterial ability [2].

Nanoparticles can be produced artificially by a variety of methods, such as photochemical, radiation, and electrochemical ones. Still, these techniques are expensive, leave harmful residues in the environment, and pollute the environment. Because of this and their high efficiency, cheap cost, eco-friendliness, and scale-up properties, natural ingredients are increasingly being considered for the synthesis of nanoparticles [3]. By utilizing green technology for nanoparticle synthesis, we can harness the potential of this existing natural treasure in an environmentally conscious way. Therefore, this eco-friendly green synthesis method benefits the pharmaceutical sector. Also, unlike conventional methods, green nanoparticle production rarely requires a lot of money or human resources. Similar to physical or chemical methods of nanoparticle manufacturing, they pose no threat to living things and are environmentally benign [4].

Soursop or *Annona muricata*, belongs to Annonaceae family which comprises around 2300 species in 130 genera. At maturity, trees reach a height of 8 to 10 m, stand upright with few branches, have rough and nut-brown stems, oblong-ovate to cylindrical leaves that range in size from 14 to 16 cm in length and 5 to 7 cm in width, and bloom at various points throughout the year on multiple trunks or branches [5]. In folk medicine, the plant is used to cure a wide range of illnesses, including skin ailments, respiratory issues, bacterial and fungal infections, fever, hyperglycaemia, hypertension, and cancer [6].

Endophytes are microscopic organisms that successfully inhabit plant tissues without causing any harm to those tissues. Every vascular plant contains endophytic organisms, which defend themselves against diseases and harmful environmental conditions by secreting bioactive secondary metabolites [7]. Certain plants produce these bioactive natural chemicals due to the co-evolution between hosts and endophytes. Endophytic fungi's physiological and ecological activities are crucial for the survival of the plants that host them and it is important to understand the diversity of symbiotic bacteria, their host or habitat despite their relative abundance as these endophytes possess significant therapeutic properties [8]. There is a common belief that medicinal plants contain endophytic fungi that produce helpful compounds.

The present investigation seeks to produce and describe silver nanoparticles (*Colleto*-AgNPs) through an aqueous endophytic extract of *Colletotrichum siamense* Prihast from *A. muricata* leaves. This research expands upon previous work that used the Quality-by-design methodology to examine the therapeutic potential of *Colleto*-AgNPs through *in-vitro* tests for antibacterial, antioxidant, and antidiabetic effects and the impact of process variables on its synthesis [9].

2 Materials and methods

2.1 Isolation and Cultivation of the Endophyte

Following our previous reports [8], the fungal endophyte was extracted from mature, healthy, and fresh *A. muricata* leaves. Its identification was verified through micro and macromorphological analysis at the Agharkar Research Institute in Pune, Maharashtra, India, affiliated with the National Fungal Culture Collection of India (NFCCI) (Supplementary File). The endophytic fungal culture that had been purified was kept in a deep freezer at -18 °C in cryovials containing Sabouraud dextrose broth that had been supplemented with 15% glycerol (v/v) [10, 11].

2.2 Synthesis of Silver Nanoparticles (AgNPs)

Sabouraud Dextrose Broth (SDB) was used to cultivate the isolated fungus for three days at 27ºC [8]. After centrifugation at 4500 rpm for 15 min, the broth was filtered through Whatman No. 1 filter paper to get a cell-free filtrate. The cell-free fungal extract was combined with 100 mL of sterile distilled water in volumes of 2 mL, 5 mL, and 8 mL, respectively, to produce the aqueous fungal extract, with the relative volumes depending on the percentage of extract needed and used for *Colleto*-AgNPs synthesis.

Following the experimental design [12, 13], a defined pH was used to add a determined amount of aqueous fungal extract [14] to a specified amount of 1 mM silver nitrate solution [15]. The mixture was allowed to react at room temperature for a predetermined reaction period. From yellow to dark brown, the color of the reaction mixture changed [12]. A 20 min centrifugation run at 10,000 rpm separated the solids from the liquid. On two or three occasions, this

centrifugation process was carried out by adding a tiny quantity of distilled water to flush out any residual contaminants. Overnight drying at 90 °C was subsequently performed on the sediment.

2.3 Statistical Experimental Design

Researchers used the Box Behnken design (BBD) to study how different formulation variables affected the size and wavelength of *Colleto*-AgNPs particles [12, 16]. We used Design-Expert® (Version 11, Stat-Ease Inc., Minneapolis, USA) to generate 27 experimental runs. We used analysis of variance (ANOVA) (F Value) to examine the effect of independent variables on the responses (Y_1: particle size and Y_2: wavelength) at three levels, specifically X_1: reductant concentration, X_2: $AgNO_3$: reducant, X_3: reaction time, and X_4: reaction pH (Table 1). The built model was analyzed using Fisher's F-test and Analysis of variance (ANOVA). The coefficient of determination, R^2, expressed the model equation's fit quality. The fitted model's correlation with the responses was then demonstrated using contour and surface plots. Contour plots and response surfaces were used to better understand the relationship and interaction between the causes and responses that were explored.

2.4 One Factor-at-a-time (OFAT) Analysis

Using OFAT, we were able to establish the ideal values for the parameters used to create silver nanoparticles. The pH, reaction time, concentration of the reductant ($AgNO_3$), and concentration of the reductant were among these parameters.

2.5 Characterization of Nanoparticles

The synthesis of *Colleto*-AgNPs was confirmed by analyzing the reaction mixture's absorption spectra with a UV-visible spectrophotometer (ThermoFisher Scientific, Orion AquaMate 8000 UV-Vis v1.007 2W2W029302, USA) over a wavelength range of 200–600 nm. A distinctive surface plasmon resonance (SPR) band in the 420–570 nm region indicated the production of AgNPs [14]. The Fourier-transform infrared spectroscopy (FTIR) was used to identify the functional groups in the produced nanoparticles, whereas the particle size and zeta potential of synthesized nanoparticles were assessed using a particle size and zeta potential analyzer (Model: Zen 3600, Malvern Instruments, Malvern, UK). An angular range of $20° < 2\theta > 80°$ was used for the powder X-ray diffraction (XRD) analysis of the produced *Colleto*-AgNPs. Energy dispersive X-ray microscopy (EDAX) was used by a scanning electron microscope (SEM) to examine the microstructure of the silver nanoparticles. A TEM analysis revealed the nanoparticles' intricate surface texture. The antibacterial activity of *Colleto*-AgNPs is strongly correlated with their size and shape [17].

Table 1 Levels of variables chosen for the experimental BBD

Independent Variables	Coded variable level		
	Low	Centre	High
	-1	0	+1
X_1: Reductant concentration (%)	2	5	8
X_2: $AgNo_3$: Reductant	1:1	1:3	1:5
X_3: Reaction time (h)	1	3	5
X_4: Reaction pH	4	7	10
Dependent Variables	**Goal**		
Y_1 : Particle size (nm)	Minimize		
Y_2: Wavelength (nm)	Minimize		

2.6 Brine Shrimp Lethality Bioassay

In order to determine whether the synthesised nanoparticles were cytotoxic, we tested them on *Artemia salina* Leach eggs [12, 16]. In brief, the initial step was to create three distinct concentrations (in geometric series) of *Colleto*-AgNPs in seawater: 1000, 100, and 10 ppm. Afterwards, 10 out of 11 shrimps were given 3 mL of each test solution. The assay was conducted in triplicate, and the control tubes contained seawater in an equivalent amount. The number of survivors was counted and the LC_{50} was determined after 24 h.

2.7 *In-vitro* Biological Assays

2.7.1 Antibacterial Assay

Silver has a lengthy history of medicinal usage in many parts of the world. Research has shown that nanosized particles of silver have enhanced antibacterial activity when contrasted with bulk silver. The antibacterial efficiency of the *Colleto*-AgNPs produced was investigated using the agar well diffusion method [16, 18]. Gram-positive bacteria such as *S. aureus* and *L. monocytogenes*, as well as gram-negative bacteria such as *E. coli* and *S. typhimurium*, were procured from the National Collection of Industrial Microorganisms (NCIM) in Pune, India.

The broth dilution procedure assessed each bacterium's minimum inhibitory concentration (MIC) before the zone of inhibition tests were conducted using *Colleto*-AgNPs solution as the test medication [19]. Individual microwells were filled with 50 µL of Mueller-Hinton (MH) broth and *Colleto*-AgNPs at several concentrations. Additionally, bacterial inoculums containing 10^6 CFU/mL of *L. monocytogenes*, *S. aureus, E. coli*, and *S. typhimurium* were introduced and

inoculated at 37ºC. Following a 24 h period of rest, 20 µL of p-iodonitrotetrazolium dye (0.5 mg/mL) was introduced and left to incubate at 37 ºC for 30 min. Streptomycin was the antibiotic of choice in both experiments.

For agar well diffusion method, the subcultures of the organisms were grown onto nutrient agar slants at 35 °C from pure cultures. A cork borer was used to make four wells of 6mm into each PCA (Plate Count Agar) plate. The spread plate method infected these plates with their respective bacterial suspensions, which were produced in normal saline. A micropipette was used to pour 20 µL of test drug solution (varying concentrations) into each well of all the bacterium plates. Variegated concentrations of streptomycin were applied to a separate set of plates that had been inoculated with the four bacteria (the positive control group). The plates were left to incubate at 30 ± 2 °C for 24 h, after which the inhibition zones were measured.

2.7.2 Antidiabetic Activity

2.7.2.1 α- Amylase Enzyme Inhibitory Assay The α-amylase enzyme inhibitory activity of *Colleto*-AgNPs was determined using the methodology described by Amalraj et al. [20]. The following amounts of *Colleto*-AgNPs were used: 50, 100, 150, 200, and 250 µg/mL. 100 µL of each concentration was combined with a starch solution (1%) that contained 20 mM phosphate buffer saline (pH 6.9) and 6 mM sodium chloride. The mixture was pre-incubated at 25ºC for 10 min followed by incubation under the same conditions after adding 100 µL of pancreatic α-amylase enzyme (0.5 mg/mL). Further, 200 µL of dinitrosalicylic acid was added and incubated at 100 ºC for 5 min to terminate the hydrolytic reaction that had been started. Acarbose served as a positive control to measure absorbance at 540 nm, and the combination was further diluted with deionized water when the samples reached room temperature. The antidiabetic ability (α-amylase enzyme) of the *Colleto*-AgNPs was calculated with the following equation,

$$\text{Inhibition}\,(\%) = \frac{\text{Absorbance of Acarbose} - \text{Absorbance of } Colleto - \text{AgNPs}}{\text{Absorbance of Acarbose}} \times 100$$

2.7.2.2 α- Glucosidase Enzyme Inhibitory Assay The method of Halarenkar et al. [21] followed in conducting the α-glucosidase enzyme inhibitory assay was used to assess the ability of *Colleto*-AgNPs to inhibit the enzyme. A mixture of 50 µL of *Colleto*-AgNPs solution in different concentrations (50, 100, 150, 200, and 250 µg/mL) and 50 µL of p-nitrophenyl-α-D glucopyranoside dissolved in phosphate buffer was prepared using sodium phosphate buffer (100 mM pH 6.9). The mixture was then incubated at 37 ºC for 5 min. Each microwell was then supplemented with 100 µL of phosphate buffer containing α-glucosidase enzyme (0.1 U/mL). We used acarbose, a typical enzyme inhibitor, to quantify the absorbance at 405 nm after 30 min of resting. The antidiabetic ability (α- glucosidase enzyme) of the *Colleto*-AgNPs was calculated with the following equation,

$$\text{Inhibition}\,(\%) = \frac{\text{Absorbance of Acarbose} - \text{Absorbance of } Colleto - \text{AgNPs}}{\text{Absorbance of Acarbose}} \times 100$$

2.7.3 Antioxidant Activity

We used the previously described approach of Raj et al. [22] to determine the DPPH radical scavenging capability of *Colleto*-AgNPs. An equal volume of DPPH solution (0.1 mM) in methanol was added to 100 µL of *Colleto*-AgNPs from various concentrations (50, 100, 150, 200, and 250 µg/mL). The mixture was incubated for 30 min at room temperature, and the absorbance was recorded at 517 nm. Ascorbic acid was used as the standard antioxidant medication, and the DPPH radical scavenging activity was measured as IC_{50} µg/mL. The antiradical ability of the *Colleto*-AgNPs was calculated with the following equation,

$$\text{Inhibition}\,(\%) = \frac{\text{Absorbance of Ascorbic acid} - \text{Absorbance of } Colleto - \text{AgNPs}}{\text{Absorbance of Ascorbic acid}} \times 100$$

2.8 Statistical Analysis

The collected results were presented as mean ± standard deviation. The IC_{50} value for enzyme inhibitory (α-amylase and α-glucosidase enzyme) and antioxidant (DPPH) experiments was obtained using non-linear regression analysis. By applying the findings to one-way ANOVA (Analysis of Variance) using Duncan's test at the 5% (%) significance level, the statistical difference or significance of the reported data was ascertained. Statistical significance was determined for reported values with $P < 0.05$, and STATISTICA 12.5 software was utilised.

3 Results and Discussion

The current investigation found that the reducing agent in the endophytic fungus *C. siamense* aqueous extract turned a dark brown color when it came into touch with the $AgNO_3$ solution. Enzymes such as reductase, nitrate reductase, and hydrogenase are being considered as potential pathways for the bio-reduction of silver. Figure S1 illustrates that the color of solution changes from colorless to pale yellow to dark brown as the reaction progresses, which is a visual signal of *Colleto*-AgNPs synthesis. When surface plasmon vibration is excited, a color shift occurs, which means silver nanoparticles are in the solution. These findings can be confirmed if the surface absorption band is located at about 420 nm, as predicted from UV-visible spectra [12]. A reducing agent is required for the bio-reduction of silver to occur; this agent is reported to have reduced Ag^+ in an $AgNO_3$ solution to Ag0 on the nanoscale, as shown in Eq. 1 [12];

$$Ag^+ + e^- \rightarrow Ag_0 \quad (1)$$

3.1 Optimization of Silver Nanoparticles

The Box Behnken Design (BBD) experiment was used to find the optimal parameters for synthesizing *Colleto*-AgNPs. The concentration of the reductant, reaction pH, duration of the reaction, and the ratio of $AgNO_3$ to reductant are the variables examined in this investigation. One possible route for AgNPs synthesis is enzymatic reduction. The nitrate reductase enzyme is commonly considered the mechanism, acting as a reducing agent. This study examined the relationship between nanoparticle formation and reductant concentration, among other parameters. The effects of independent factors on the response variables were examined using BBD. These variables were reductant concentration (X_1), $AgNO_3$: reductant (X_2), reaction time (X_3), and reaction pH (X_4). The experimental runs for BBD were 27 in total, and Table 2 shows the resulting matrix of variables with examined levels and practical responses, including particle size (Y_1) and wavelength (Y_2).

The values for Y_1 and Y_2 responses spanned from 95.32 to 119.64 nm and 401 to 430 nm, respectively, as outlined in Table 2. The Quadratic model emerged as the optimal fit for both Y_1 (R^2: 0.9518 and PRESS: 408.02) and Y_2 (R^2:

Table 2 BBD matrix runs with results of response variables (Independent and dependent variables)

Std	Run	X_1: Reductant concentration (%)	X_2:$AgNO_3$:Reductant	X_3:Reaction time (hr)	X_4:Reaction pH	Y_1 Particle size (nm)	Y_2 Wavelength
24	1	5	5	3	10	104.45	408
7	2	5	3	1	10	98.12	402
10	3	8	3	3	4	99.04	402
26	4	5	3	3	7	115.65	419
18	5	8	3	1	7	98.2	401
13	6	5	1	1	7	97.42	402
17	7	2	3	1	7	97.68	408
8	8	5	3	5	10	119.64	415
2	9	8	1	3	7	103.36	408
16	10	5	5	5	7	105.94	414
25	11	5	3	3	7	114.49	419
6	12	5	3	5	4	102.48	402
23	13	5	1	3	10	117.73	401
14	14	5	5	1	7	101.46	402
15	15	5	1	5	7	113.59	420
5	16	5	3	1	4	100.27	402
3	17	2	5	3	7	97.45	407
11	18	2	3	3	10	98.62	401
20	19	8	3	5	7	111.04	421
1	20	2	1	3	7	99.35	412
22	21	5	5	3	4	100.64	400
4	22	8	5	3	7	99.41	401
27	23	5	3	3	7	117.73	416
21	24	5	1	3	4	100.07	402
19	25	2	3	5	7	95.32	407
9	26	2	3	3	4	101.38	408
12	27	8	3	3	10	114.63	430

0.8137 and PRESS: 1814.94). This suggests that the chosen model is adept at predicting 95.18% and 81.37% variations in the dependent variables Y_1 and Y_2, respectively. Further affirmation of the model's significance was sought through ANOVA, as detailed in Table S1. The response Y_1 and Y_2 values ranged between 97.45 and 144.45 and 406–431 nm, respectively (Table 2). The Quadratic model was best fit for both Y_1 (R^2 0.9438 and PRESS: 1412.36) and Y_2 (0.8616 and PRESS: 1666.14). Based on this, it can be corroborated that the selected model can accurately predict 94.38 and 86.16% changes in dependent variables Y_1 and Y_2, respectively. ANOVA was used further to determine the model's significance (Table S1).

F values of 14.39 and 8.49 for responses Y_1 and Y_2 corroborate the model's significance. Predicted R^2 values of 0.70 and 0.57 for Y_1 and Y_2 did not differ by more than 0.2 from adjusted R^2 of 0.88 and 0.76, respectively. This confirms reasonable agreement between the two values. Plotting observed and predicted values verified the significance of both quadratic models (Figure S2). The relationship between independent and dependent variables can be studied using the following equations,

$$\begin{aligned} Y_1 = {} & +140.28 + 3.74X_1 + 2.29X_2 + 0.8183X_3 \\ & + 7.71X_4 - 2.86X_1X_2 - 0.9625 \\ & X_1X_3 + 7.30X_1X_4 + 0.1125 \\ & X_2X_3 - 0.6100X_2X_4 + 7.69X_3X_4 - 13.23{X_1}^2 \\ & - 21.71{X_2}^2 - 15.07{X_3}^2 - 8.43{X_4}^2 \end{aligned} \quad (2)$$

$$\begin{aligned} Y_2 = {} & +435.33 - 0.3333X_1 - 0.2500X_2 \\ & - 0.8333X_3 + 8.08X_4 + 1.0000X_2X_3 + 0.5000X_2X_4 \\ & + 1.50X_3X_4 - 18.17{X_1}^2 - 15.04{X_2}^2 - 14.67{X_3}^2 - 8.79{X_4}^2 \end{aligned} \quad (3)$$

X_1 showed a significant positive effect on Y_1, while X_4 showed substantial positive impacts on Y_1 and Y_2. Terms $X_1 \times_4$ and $X_3 \times_4$ exhibited significant positive effects on Y_1. The quadratic term of each factor (X_1 to X_4) significantly negatively affected both responses. 3D response surface plots were used to validate these results further (Fig. 1).

Two-factor interactions ($X_1 \times_4$ and $X_3 \times_4$) were further confirmed by the crossed lines observed in interaction plots (Figures S2 and S3). Figure S4 shows model diagnosis plots, which include a normal and residual versus run plot. On critically observing these plots, it can be inferred that residuals followed a straight line, signifying an even distribution of errors. The residuals versus run plot similarly demonstrated a random dispersion.

3.2 Model Validation

Software suggested that optimized values, i.e., 5.079% of reductant concentration, 1:1.23 ratio of $AgNO_3$: Reductant with a reaction time of 1.15 h and pH value of 8.77, will produce optimized formulation. The region of optimized formulation is depicted in Figure S5. The predicted particle size and wavelength values were 105.86 nm and 413.5 nm, respectively. Predicted and actual results were in close agreement, indicating the model's validity.

3.3 Optical Characterization by UV-visible Absorption

One simple and effective way to verify the creation of nanoparticles is by using UV-visible absorption spectroscopy. The UV-visible absorption spectra of the optimized batch of AgNPs, as per the Box Behnken Design, are displayed in Fig. 2. A wide absorption band from 300 to 500 nm and a maximum at 420 nm in the spectra point to the presence of *Colleto*-AgNPs.

3.4 Microscopic Analysis by SEM with EDAX and TEM Studies

In Fig. 3, the morphological examination results of the produced *Colleto*-AgNPs are shown in both the SEM examinations (Fig. 3A) and the EDAX spectra (Fig. 3B). Both the TEM and SAED analyses indicated that the nanoparticles had a spherical form (Fig. 3C and D). Applying EDAX analysis improves the identification of the minerals in the synthesized nanoparticles. The produced silver nanoparticles were discovered to include several minerals, including calcium, silver, carbon, and oxygen, according to EDAX analysis. The pre-analysis sample treatment is responsible for the presence of gold and palladium in the results.

3.5 Structural Analysis

The XRD pattern of the finished *Colleto*-AgNPs in the 2Θ range of 20º-80º is displayed in Fig. 3E. The *Colleto*-AgNPs exhibited diffraction peaks at 38.1º, 44.35º, 64.5º, and 77.48º, as recorded by the XRD peaks. A strong peak at 38.10º diffraction suggested that the silver crystal was perpendicular to the plane. A mean particle size of 16.16 nm was determined for the produced nanoparticles using the following formula:

$$D = 0.9\lambda/\beta cos\theta$$

where D is the crystalline size, λ is the X-ray wavelength (CuKa / 1.541862 A), β is the full width at half maximum, and Θ is Bragg's angle.

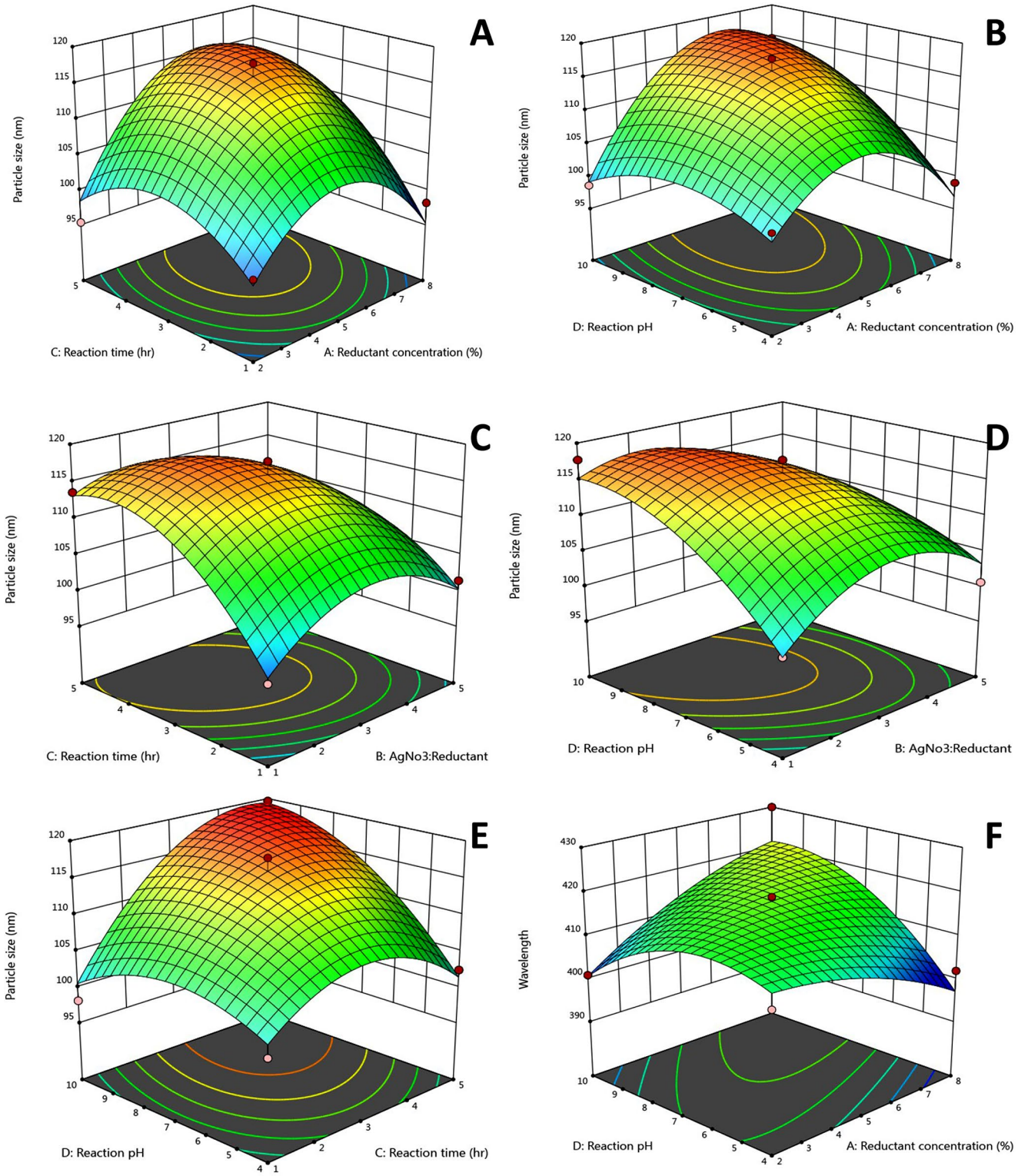

Fig. 1 3D response surface plots showing the effect of variables on response Y_1 (A-E) and Y_2 (F)

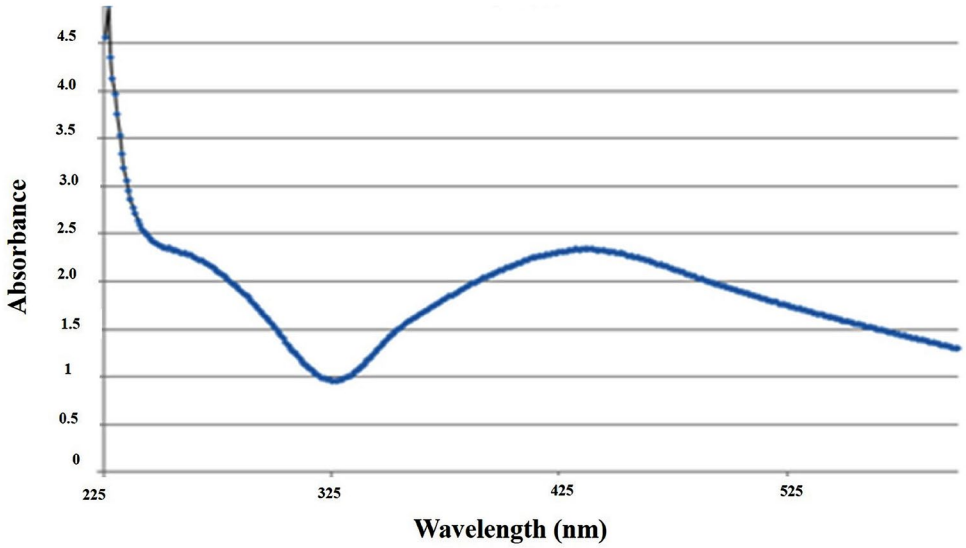

Fig. 2 UV-visible spectra of *Colleto*-AgNPs at reductant concentration:- 7.664%, $AgNO_3$: Reductant ratio :- 1:3.122, reaction time :- 3.271 h, and reaction pH :- 10, showing an absorption peak at 420 nm

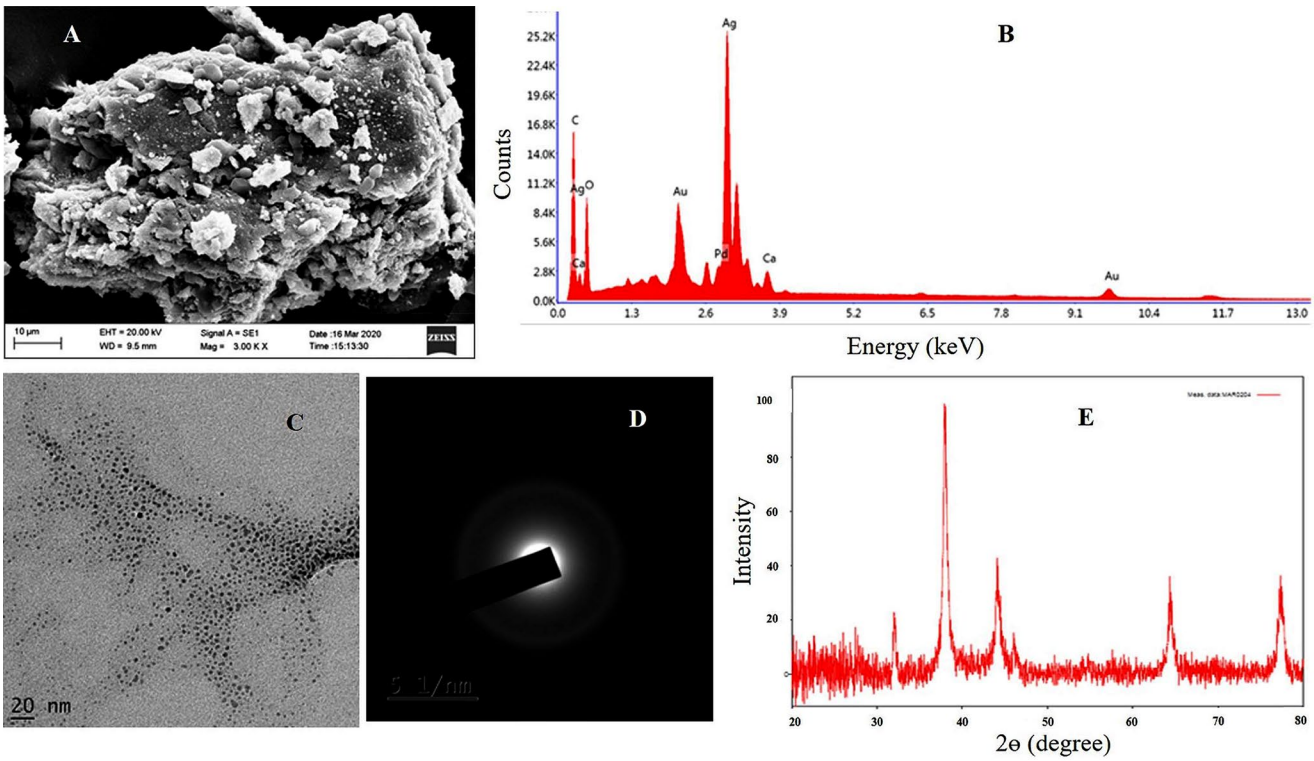

Fig. 3 (**A**) SEM, (**B**) EDAX, (**C**) TEM (**D**) SAED (**E**) XRD analysis of *Colleto*-AgNPs

3.6 Particle Size Analysis

The average particle size was found to be 98.48 nm (Fig. 4A), and the polydispersity index (PDI) was 0.198 with a zeta potential of -4.92 mV (Fig. 4B). Particle characteristics shown in Fig. 4 include a mobility of -1.626e-004 cm^2/Vs, a Doppler shift of 12.84 Hz, a base frequency of 127.3 Hz, and a conductivity of 0.3243 mS/cm.

3.7 Cytotoxicity Study by Brine Shrimp Lethality Bioassay

The cytotoxic effect of synthesized *Colleto*-AgNPs was investigated using a brine shrimp lethality experiment with varying nanoparticle doses for 24 h. Results revealed that brine shrimps were highly susceptible to *Colleto*-AgNPs, even at lower doses. Since the LC_{50} falls within the range of 100 to 1000 ppm, the *Colleto*-AgNPs were determined

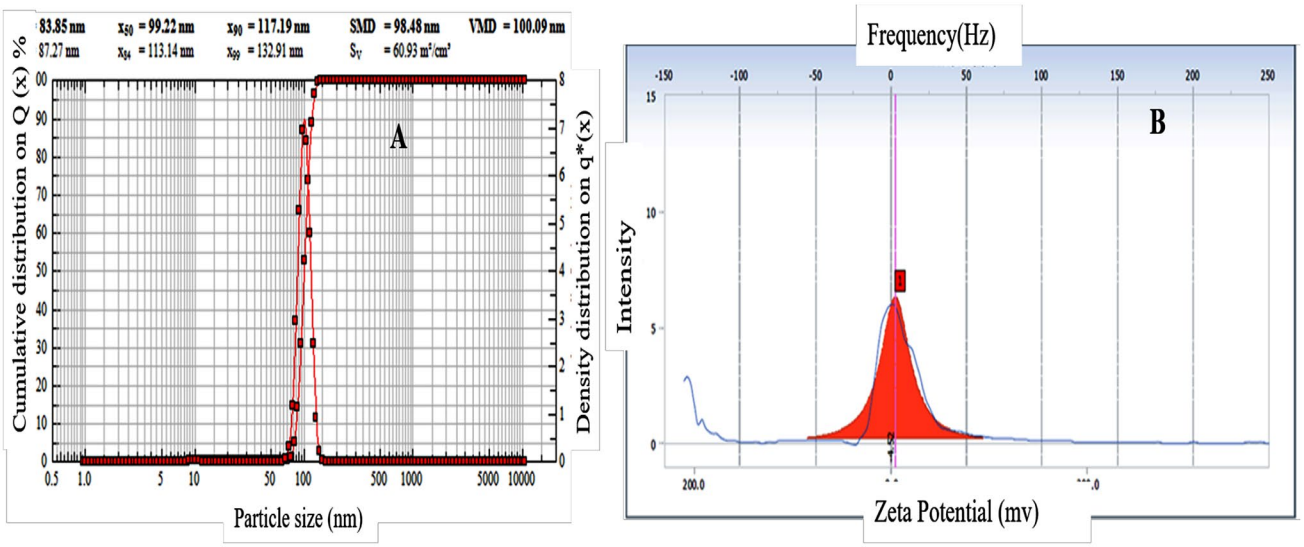

Fig. 4 (**A**) Particle size and (**B**) Zeta potential analysis of the synthesized *Colleto*-AgNPs

Table 3 Minimum inhibitory concentration (MIC) of *Colleto*-AgNPs

Samples	Minimum inhibitory concentration (µg/mL)			
	E. coli	*L. monocytogenes*	*S. aureus*	*S. typhimurium*
A. muricata leaf extract	375	187.5	93.75	> 750
C. siamense (Endophyte) extract	750	375	187.5	> 750
Colleto-AgNPs	187.5	46.87	23.43	> 750
Streptomycin	11.7	2.9	2.9	5.8

to have an LC_{50} value of 312.51 ± 32.54 and could exhibit some biological activity. $KCrO_7$ solution (positive control) showed $LC_{50} < 10$ µg/mL, whereas no deaths were observed in seawater (negative control). Our results were in agreement with the cytotoxic efficacy of nanoparticles reported by Gawas et al. [16].

3.8 In-vitro Antibacterial Activity

Microbial diseases pose serious health threats, and the emergence of multidrug-resistant microbes necessitates the development of new effective techniques. Nanotechnology offers a novel approach to combat these diseases by utilizing the antimicrobial properties of nanomaterials, which interact easily with microbial cells to exhibit their mechanisms [23]. AgNPs are considered an essential type of metallic nanoparticles due to their antibacterial properties and their ability to form silver salts (Ag) by reduction, and they are unique in having an increased surface area to volume ratio [24]. These properties make them suitable in diverse areas like biomedicine, catalysis, pharmaceuticals, and biosensors. Silver has a long history of being used as an antimicrobial agent in treating *Neisseria gonorrhoeae* [25]. Compared to Ag, the usage of AgNPs has increased due to its substantial surface area. Green synthesized AgNPs have proven their efficacy as an efficient antioxidant, antibacterial, anticancer, antidiabetic, photocatalytic, and mosquitocidal agent [26].

The study adopted the microdilution method to determine the minimum inhibitory concentration (MIC) of *Colleto*-AgNPs and was reported to be highly effective in suppressing *E. coli, L. monocytogenes, S. aureus*, and *S. typhimurium* at the dosage of 23.43, 46.87, 187.5 and > 750 µg/mL (Table 3). The study found that *E. coli* was slightly resistant to *Colleto*-AgNPs and the standard antibiotic, streptomycin, as it required a high concentration of 187.5 and 11.7 µg/mL, respectively. The leaf extract of *A. muricata* required an increased amount of > 750, 375, 187.5, and 93.75 µg/mL to inhibit or kill *S. typhimurium, E. coli, L. monocytogenes*, and *S. aureus.* While at > 750, 750, 375, and 187.5 µg/mL concentrations, the fungal extract of *C. siamense* inhibited *S. typhimurium, E. coli, L. monocytogenes*, and *S. aureus.*

In the disc diffusion method, at a concentration of 750 µg/mL, *Colleto*-AgNPs exhibited the strongest inhibitory action against *L. monocytogenes* (23.98 mm), and then against *S. aureus* (22.9 mm), *E. coli* (20.23 mm) and *S. typhimurium* (17.76 mm). From Table 4, it is evident that the conventional antibiotic streptomycin exhibited the highest zone of inhibition by inhibiting the growth of *L. monocytogenes* (25.02 mm), followed by *S. typhimurium* (23.52 mm), *S. aureus* (23.34 mm), and *E. coli* (22.21 mm). Accordingly, the fungal endophyte synthesized silver nanoparticles can be considered an appropriate broad-spectrum antimicrobial as they have exhibited better antibacterial activity against the studied microorganisms even at a low 125 µg/mL concentration.

Table 4 Antibacterial activity of *Colleto*-AgNPs against pathogenic bacteria

Samples	Concentration (µg/mL)	Zone of inhibition (mm)			
		S. aureus	*L. monocytogenes*	*E. coli*	*S. typhimurium*
A. muricata leaf extract	125	13.67 ± 1.34	15.81 ± 0.41	11.0 ± 0.13	13.3 ± 0.50
	250	14.14 ± 0.49	17.05 ± 1.18	13.4 ± 1.12	14.1 ± 0.28
	500	17.61 ± 0.16	20.38 ± 0.56	15.1 ± 0.51	16.2 ± 0.71
	750	19.71 ± 0.09	22.13 ± 0.00	17.9 ± 0.79	18.0 ± 0.22
C. siamense (Endophyte) extract	125	11.89 ± 0.29	13.13 ± 1.79	9.51 ± 0.23	8.60 ± 0.13
	250	13.40 ± 0.50	15.40 ± 0.28	11.13 ± 0.17	10.0 ± 0.81
	500	14.73 ± 0.33	16.11 ± 1.42	12.91 ± 0.28	12.31 ± 0.15
	750	15.12 ± 0.14	19.23 ± 1.28	14.60 ± 0.41	14.12 ± 0.52
Colleto-AgNPs	125	17.1 ± 0.41	19.02 ± 0.5	13.33 ± 1.11	11.12 ± 0.71
	250	19.2 ± 0.93	20.32 ± 0.0	16.14 ± 1.54	12.33 ± 1.35
	500	22.5 ± 1.16	22.45 ± 0.7	18.66 ± 1.13	14.41 ± 1.56
	750	22.9 ± 1.72	23.98 ± 1.2	20.23 ± 0.52	17.76 ± 1.94
Streptomycin	30	23.34 ± 0.73	25.02 ± 1.4	22.21 ± 1.5	23.52 ± 0.00

Values were expressed as mean ($n = 3$) ± standard deviation

At the high concentration, *Colleto*-AgNPs activity was similar to streptomycin in inhibiting the growth of *S. aureus* and *L. monocytogenes*. The study also estimated the antibacterial activity of *A. muricata* leaf extract and *C. siamense* (endophyte) extract. The zone of inhibition produced by *A. muricata* leaf extract ranged from 17.9 mm to 22.13 mm, and the zones produced by *C. siamense* (endophyte) extract ranged between 14.12 mm and 19.23 mm. The antibacterial activity of these extracts was less compared to the activity of *Colleto*-AgNPs and streptomycin (Table 4). In the present study, the *Colleto*-AgNPs have expressed noteworthy antibacterial activity against *S. typhimurium*, *L. monocytogenes*, and *E. coli.*

According to NajeerAhamed et al. [27] the AgNPs synthesized using *Colletotrichum gloeosporioides* have shown reduced antibacterial activity by forming inhibitory zones of diameter 14 and 15 mm against *E. coli* (ATCC 25,922) at the concentration of 25 and 50 µg/mL and against MDR 1 and MDR 2 strains of *E. coli*, the zone of inhibition formed by 25 and 50 µg/mL of *C. gloeosporioides* mediated AgNPs was in the range between 12 and 15 mm [23]. The AgNPs synthesized from *Penicillium* isolated from the leaves of *Curcuma longa* have shown their antibacterial property by forming zone of inhibition of 14 mm and 13 mm against *S. typhimurium* and *E. coli* at the dosage of 80 µg/mL [28].

The silver nanoparticles synthesized from the aqueous extracts of *Nigella sativa* revealed very poor bacterial inhibitory activity even at higher concentration with the inhibition zones of 16.45, 17.38, and 14.35 mm against the bacterial strains *E. coli*, *S. aureus* and *S. typhimurium*, respectively [29]. The difference in the antibacterial activity exhibited by *Colleto*-AgNPs is due to the structural variation among the gram-positive and gram-negative bacteria. The AgNPs exhibit their antibacterial activity by disrupting the cell walls and membranes, altering the cell membrane's permeability, impairing proteins, inhibiting DNA replication, and increasing the production of reactive oxygen species, which results in oxidative stress [30].

The nanoaparticle also causes denaturation and dysfunctioning of ribosomes and mitochondria. It is fascinating that these AgNPs release or produce toxic silver ions to bacterial organisms, disrupting the physiological processes and damaging the cell components (Fig. 5) [24]. The increased surface-to-volume ratio nature of AgNPs also influences their antibacterial activity. Compared with the previously synthesized AgNPs, the antibacterial efficacy of AgNPs (*Colleto*-AgNPs) synthesized using *Colletotrichum siamense* is remarkable.

3.9 *In-vitro* Antidiabetic Activity

Diabetes is a multifactorial disease characterized by elevated blood glucose levels, aberrant pancreatic insulin production, or insulin resistance in peripheral tissues [31]. The pancreatic α-amylase and intestinal α-glucosidase enzymes, which break down carbs, are known to have a role in the development of diabetes by elevating postprandial glucose levels. The kidney and liver are negatively impacted by miglitol, acarbose, and voglibose that inhibit the activity of α-amylase and α-glucosidase enzymes. These enzymes, located in brush borders of intestinal absorptive cells, hydrolyses the non-absorbable polysaccharides and oligosaccharides into absorbable monosaccharides (Fig. 6) [32]. Hence, finding robust α-amylase and α-glucosidase inhibitors in diabetes patients that are safe and derived from natural sources is of utmost importance. The effect of *Colleto*-AgNPs on blood sugar levels was assessed in this study using enzyme inhibition assays of α-amylase and α-glucosidase.

In the current investigation, the standard drug used was acarbose, which partially required a IC_{50} of 25.07 ± 0.21 µg/

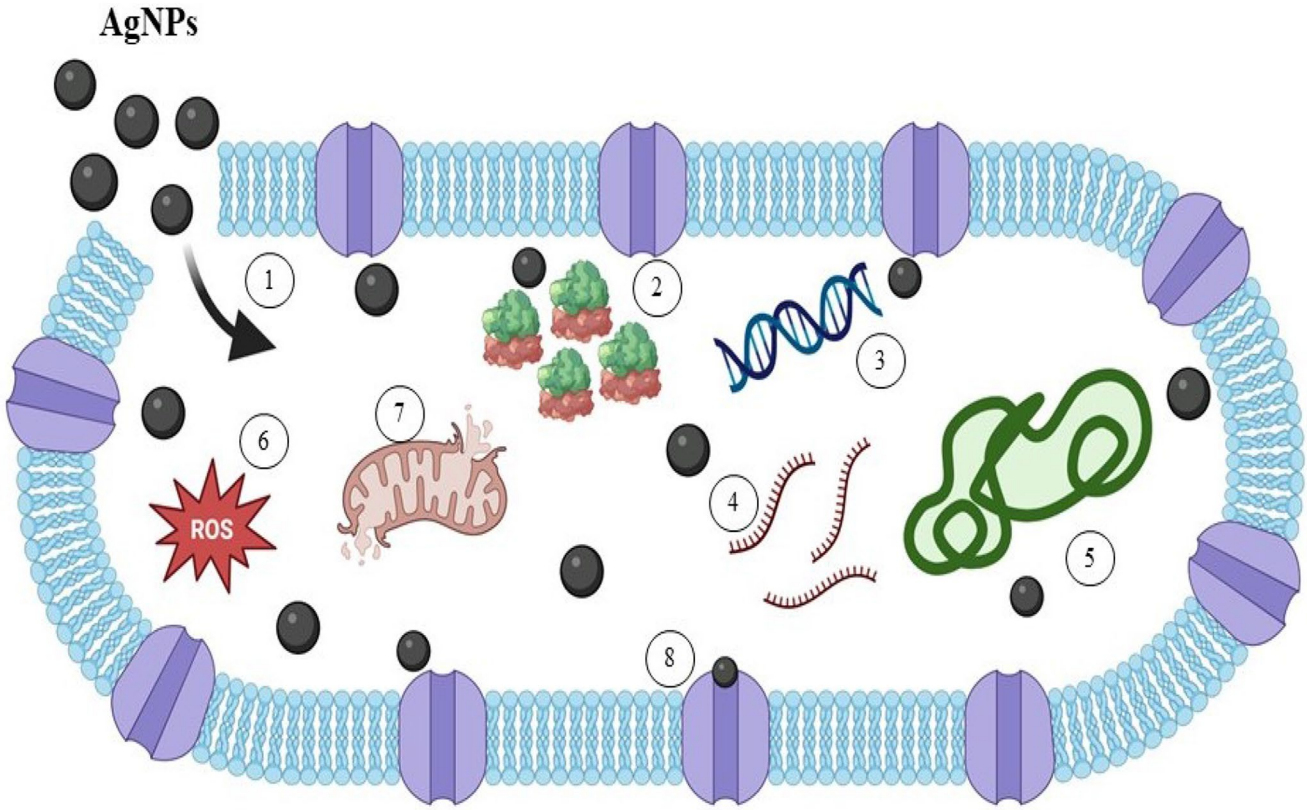

Fig. 5 The possible antibacterial mechanism exhibited by AgNPs include disruption of cell wall and cell membrane (1), denaturation of ribosomes (2), disruption of DNA replication (3), denaturation of RNA (4) and proteins (5), generation of ROS (6), mitochondrial dysfunction (7) and disruption of electron transport chain (8)

mL concentration to inhibit the 50% α-amylase enzyme concentration (Table 5). The study evaluated the enzyme inhibitory property of *A. muricata* leaf extract, *C. siamense* (endophyte) fungal extract, and *Colleto*-AgNPs on comparison with acarbose under various concentrations (50, 100, 150, 200, and 250 µg/mL). Compared to the α-amylase enzyme inhibition activity of *A. muricata* leaf extract and the fungal extract of *C. siamense*, the activity of the nanoparticle synthesized (*Colleto*-AgNPs) using *C. siamense* was superior with IC_{50} of 30.57 ± 0.17 µg/mL, while the former exhibited activity with the IC_{50} of 51.19 ± 0.82 and 47.43 ± 0.71 µg/mL.

Like the results of α-amylase enzyme inhibitory activity, finer results were demonstrated by *Colleto*-AgNPs against α-glucosidase enzyme with an IC_{50} of 32.30 ± 1.23 µg/mL. The individual extracts of *A. muricata* leaves and *C. siamense* endophytic fungus extract required IC_{50} of 49.08 ± 0.09 and 44.19 ± 0.52 µg/mL to cause partial inhibition of α-glucosidase enzyme. The standard drug acarbose showed remarkable activity with IC_{50} of 24.16 ± 0.44 µg/mL. Ishnava et al. [32] evaluated the α-amylase inhibition activity of AgNPs synthesized using *Enicostema axillare* leaf extract. This nanoparticle has revealed good inhibition of about 70% with a least 10 µg/mL concentration. The AgNPs synthesized with *Hybanthus enneaspermus* had less α-amylase and α-glucosidase enzyme inhibitory activity compared to the results of *Colleto*-AgNPs, IC_{50} exhibited by AgNPs was 41.27 ± 0.11 and 42.87 ± 0.44 µg/mL, respectively [33].

3.10 *In-vitro* Antioxidant Activity

The reactive molecules comprising reactive oxygen species (ROS) and reactive nitrogen species (RNS) are the byproducts of a biological system. These reactive molecules or species are also considered signaling molecules [34]. The molecular network interaction established by these ROS and RNS between the signaling pathways of ROS and RNS plays a vital role in regulating stress responses. Human body contain non-enzymatic antioxidants and enzymatic natural antioxidants to balance the reactive molecules. However, an increased population of these free radicals destroys the antioxidant defence system in humans, which eventually results in oxidative stress by damaging the DNA, proteins, and lipids and alters the cell structure [7] (Fig. 7). In adverse

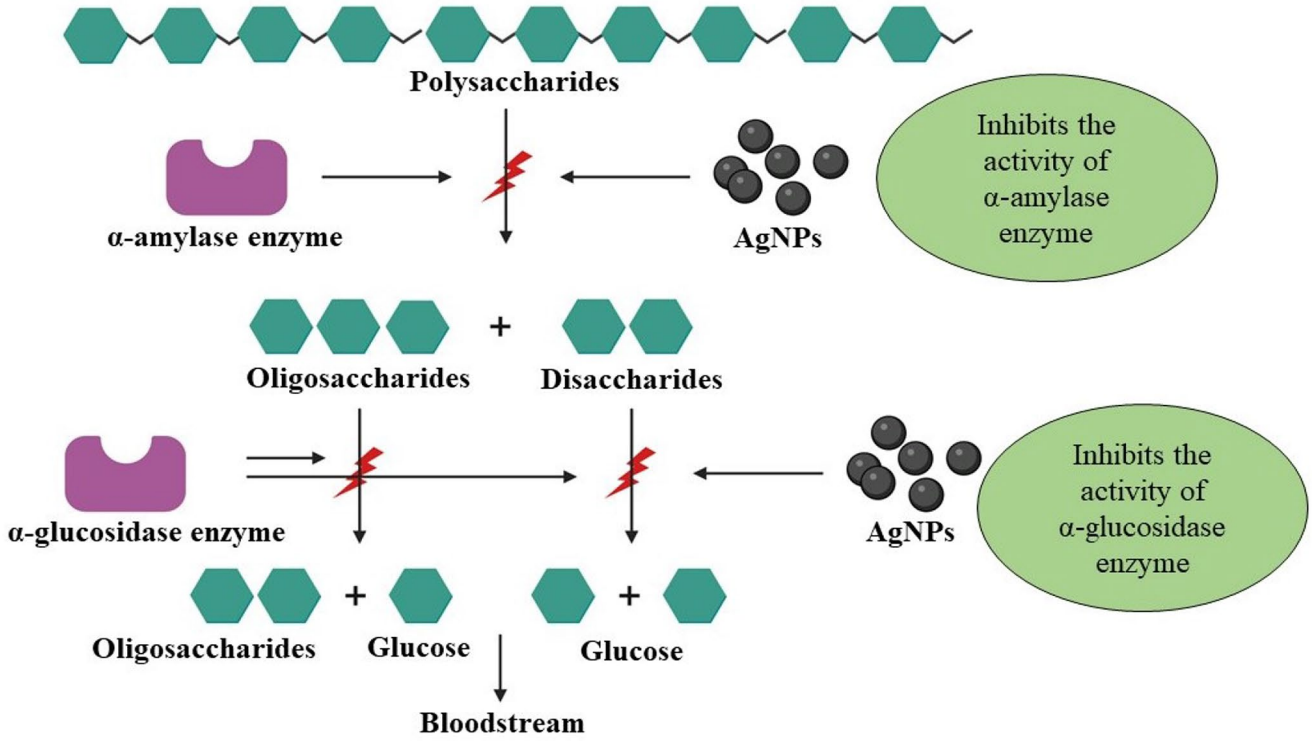

Fig. 6 Possible antidiabetic mechanism of AgNPs through the breakdown of polysaccahrides, oligosaccharides, and disaccharides that inhibits the activity of α-amylase and α-glucosidase enzymes

Table 5 *In-vitro* antidiabetic and antioxidant activity of *A. muricata* leaf extract, *C. siamense* extract, and *Colleto*-AgNPs

Test drugs	α-amylase enzyme inhibition assay	α-glucosidase enzyme inhibition assay	DPPH free radical scavenging assay
A. muricata leaf extract (IC_{50} µg/mL)	51.19 ± 0.82	49.08 ± 0.09	38.13 ± 0.13
C. siamense (Endophyte) extract (IC_{50} µg/mL)	47.43 ± 0.71	44.19 ± 0.52	31.38 ± 0.09
Colleto-AgNPs (IC_{50} µg/mL)	30.57 ± 0.17	32.30 ± 1.23	26.98 ± 0.30
Standard (IC_{50} µg/mL)	25.07 ± 0.21[#]	24.16 ± 0.44[#]	16.14 ± 0.21[$]

Values are expressed as mean ($n = 3$) ± standard deviation. # - Acarbose; $ - Ascorbic acid

conditions, they induce brain injury, cardiovascular and neurodegenerative diseases, and sepsis [35].

The present study estimated the free radical scavenging activity of *Colleto*-AgNPs against the DPPH radical. DPPH is a stable molecule soluble in methanol solvent and has a maximum absorption at 517 nm. The *Colleto*-AgNPs have displayed higher antioxidant activity by scavenging the DPPH radical with an IC_{50} of 26.98 ± 0.30 µg/mL, and the standardized antioxidant, ascorbic acid has exhibited IC_{50} of 16.14 ± 0.21 µg/mL (Table 5). The leaf and fungal extract displayed reduced antioxidant activity compared to the *Colleto*-AgNPs with IC_{50} of 38.13 ± 0.13 and 31.38 ± 0.09 µg/mL. The biosynthesized AgNPs from *Astragalus flavesces* leaf extracts exhibited efficient radical scavenging potential to a degree that it is recommended for its usage in food and pharmaceutical industries [36]. Similarly, our results were also higher and close to commercial standard control (IC_{50} 16.14 ± 0.21 µg/mL) with the IC_{50} 26.98 ± 0.30 µg/mL. A study by Geyesa et al. [24] revealed that the AgNPs synthesized using leaf extract of *Verbascum sinaiticum* required extremely high IC_{50} of 216 µg/mL to scavenge DPPH radical. With this, it can be determined that the AgNPs synthesized using *C. siamense* efficiently scavenged the DPPH radical.

4 Conclusion

Green synthesis has paved the way for simple, cost-effective, and non-toxic methods of producing nanoparticles for various uses. Plant extracts and microbial or fungal extracts are superior agents for reducing and stabilising noble metals in their respective ionic forms, allowing the metals to finally form nanoparticles through a stabilised colloidal system. The current work created an effective biosynthesis approach for silver nanoparticles that uses *Colletotrichum siamense* fungal extract as a reducing and stabilising

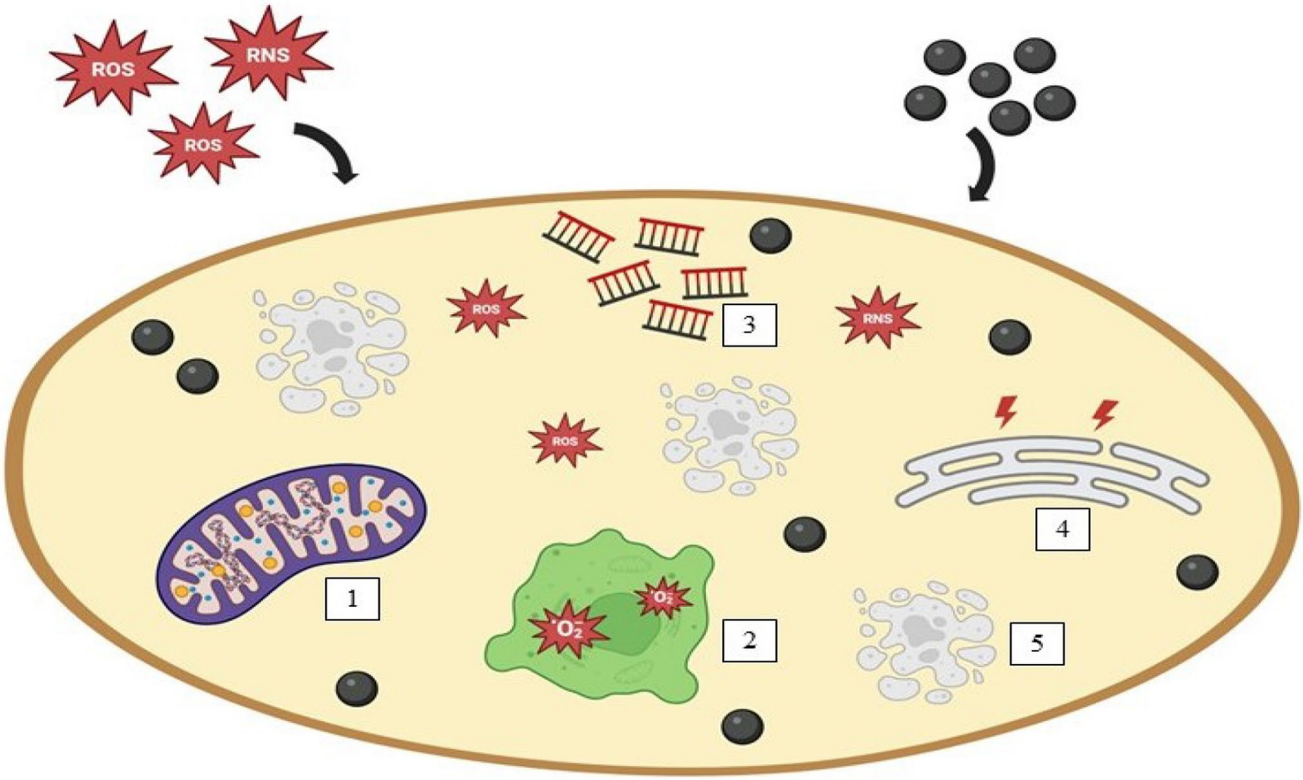

Fig. 7 Possible antioxidant mechanism of AgNPs by inhibiting the dysfunction of mitochondria (1), reducing the oxidative stress (2), inhibiting DNA fragmentation (3) and stress on endoplasmic reticulum (4), and apoptosis (5) caused by ROS and RNS

agent. Antibacterial activity against the tested gram-positive and gram-negative bacterial strains was demonstrated by the biosynthesized *Colleto*-AgNPs, which exhibited a well-defined zone of inhibition. Biogenic *Colleto*-AgNPs have also shown promising antidiabetic activity against α-amylase and α-glucosidase enzymes. At a lower dosage, *Colleto*-AgNPs could scavenge DPPH free radicals. These results shed light on the potential biological uses of *Colleto*-AgNPs, which is very important. This study is noteworthy because no previous research has shown that *C. siamense* extract may be used to make nanoparticles of silver or other metal oxides. *C. siamense* may have future use in medicine since the results show that it is an effective reducing agent for making AgNPs. However, to ascertain the effectiveness of *Colleto-AgNPs*, a comprehensive investigation of experimental animal models is necessary.

Supplementary Information The online version contains supplementary material available at https://doi.org/10.1007/s10904-024-03235-9.

Acknowledgements The authors acknowledge the generous support from the Research Supporting Project (RSP2024R352) by King Saud University, Riyadh, Kingdom of Saudi Arabia.

Author Contributions FA and CJ: Methodology, Investigation, Data curation, Original draft writing. SN: Software, formal analysis, investigation. NG, MK and RB: Formal analysis, Software, Validation, Review, and editing. MSK and SB: Formal analysis, Funding acquisition, Validation, MA and SG: Methodology, Supervision, Writing-Original draft, Review, and editing.

Data Availability No datasets were generated or analysed during the current study.

Declarations

Ethical Approval The authors declare that the manuscript has not been published previously.

Competing Interests The authors declare no competing interests.

References

1. A.S. Abdelsattar, A.G. Kamel, A.H. Hussein, M. Azzam, S. Makky, N. Rezk, K. Essam, M.M. Agwa, A. El-Shibiny, The promising antibacterial and anticancer activity of green synthesized zinc nanoparticles in combination with silver and gold nanoparticles. J. Inorg. Organomet. Polym Mater. **33**(7), 1868–1881 (2023)
2. A.Y. Yassin, A.M. Abdelghany, R.S. Salama, A.E. Tarabiah, Structural, optical and antibacterial activity studies on CMC/PVA blend filled with three different types of green synthesized ZnO nanoparticles. J. Inorg. Organomet. Polym Mater. **33**(7), 1855–1867 (2023)

3. E.N. Gecer, Green synthesis of silver nanoparticles from *Salvia aethiopis* L. and their antioxidant activity. J. Inorg. Organomet. Polym Mater. **31**(11), 4402–4409 (2021)
4. A. Elbrolesy, Y. Abdou, F.A. Elhussiny, R. Morsy, Novel green synthesis of UV-sunscreen ZnO nanoparticles using *Solanum lycopersicum* fruit extract and evaluation of their antibacterial and anticancer activity. J. Inorg. Organomet. Polym Mater. **33**, 3750–3759 (2023)
5. A.B. Sanusi, Mohd Fadzelly, Soursop—*Annona muricata*, in *Exotic Fruits Reference Guide*, ed. by S. de Oliveira Silva, E. de Brito, E.S., (Academic: Johor Malaysia, Rodrigues, 2018), pp. 391–395
6. M. Mutakin, R. Fauziati, F.N. Fadhilah, A. Zuhrotun, R. Amalia, Y.E. Hadisaputri, Pharmacological activities of Soursop (*Annona muricata* Lin). Molecules. **27**(4), 1201 (2022)
7. F. Andrade, C. Jenipher, N. Gurav, S. Nadaf, M.S. Khan, N. Mahajan, D. Bhagwat, M. Kalaskar, R. Chikhale, R. Bhole, S. Lalsare, Endophytic fungi-assisted biomass synthesis of eco-friendly formulated silver nanoparticles for enhanced antibacterial, antioxidant, and antidiabetic activities. J. Drug Deliv. Sci. Technol. **97**, 105749 (2024)
8. F. Andrade, M. Kawale, M. Ayyanar, N. Gurav, M. Kalaskar, S. Gurav, Anatomy, micromorphology, physicochemical analysis, and isolation of fungal endophytes from the leaves of *Annona muricata* L.(Annonaceae). Vegetos. **36**, 634–642 (2023)
9. J.N. Meyer, C.A. Lord, X.Y. Yang, E.A. Turner, A.R. Badireddy, S.M. Marinakos, A. Chilkoti, M.R. Wiesner, M. Auffan, Intracellular uptake and associated toxicity of silver nanoparticles in *Caenorhabditis elegans*. Aquat. Toxicol. **100**, 140–150 (2010)
10. A. Idris, I. Al-tahir, E. Idris, Antibacterial activity of endophytic fungi extracts from the medicinal plant *Kigelia africana*. Egypt. Acad. J. Biol. Sci. G Microbiol. **5**, 1–9 (2013)
11. G. Vinayarani, H. Prakash, Fungal endophytes of turmeric (*Curcuma longa* L.) and their biocontrol potential against pathogens *Pythium aphanidermatum* and *Rhizoctonia solani*. World J. Microbiol. Biotechnol. **34**, 1–17 (2018)
12. C. Dias, M. Ayyanar, S. Amalraj, P. Khanal, V. Subramaniyan, S. Das, S. Gurav, Biogenic synthesis of zinc oxide nanoparticles using mushroom fungus cordyceps militaris: characterization and mechanistic insights of therapeutic investigation. J. Drug Deliv. Sci. Technol. **73**, 103444 (2022)
13. A.S. Souza, W.N. Dos Santos, S.L. Ferreira, Application of Box–Behnken design in the optimisation of an on-line pre-concentration system using knotted reactor for cadmium determination by flame atomic absorption spectrometry. Spectrochimica Acta B at. Spectrosc. **60**, 737–742 (2005)
14. B. Ajitha, Y.A.K. Reddy, P.S. Reddy, Biogenic nano-scale silver particles by *Tephrosia purpurea* leaf extract and their inborn antimicrobial activity. Spectrochimica Acta A: Mol. Biomol. Spectrosc. **121**, 164–172 (2014)
15. S. Priya, K. Murugan, A. Priya, D. Dinesh, C. Panneerselvam, G.D. Devi, B. Chandramohan, P.M. Kumar, D. Barnard, R. Xue, Green synthesis of silver nanoparticles using *Calotropis gigantea* and their potential mosquito larvicidal property. Int. J. Pure Appl. Zool. **2**, 128–137 (2014)
16. G. Gawas, M. Ayyanar, N. Gurav, D. Hase, V. Murade, S. Nadaf, M.S. Khan, R. Chikhale, M. Kalaskar, S. Gurav, Process optimization for the Bioinspired synthesis of gold nanoparticles using *Cordyceps Militaris*, its characterization, and Assessment of enhanced therapeutic efficacy. Pharmaceuticals. **16**, 1311 (2023)
17. M.D. Mashitah, Y. San Chan, J. Jason, (2016) Antimicrobial properties of nanobiomaterials and the mechanism. *Nanobiomaterials in Antimicrobial Therapy*; Elsevier, 261–312
18. M. Nilavukkarasi, S. Vijayakumar, M. Kalaskar, N. Gurav, S. Gurav, P. Praseetha, *Capparis Zeylanica* L. conjugated TiO_2 nanoparticles as bio-enhancers for antimicrobial and chronic wound repair. Biochem. Biophys. Res. Commun. **623**, 127–132 (2022)
19. G. Slavika, M. Ayyanar, P. Gangapriya, M. Kalaskar, V. Redasani, N. Gurav, S. Nadaf, M. Deshpande, R. Bhole, S. Gurav, Fabrication of chitosan nanocomposites loaded with biosynthetic metallic nanoparticles and their therapeutic investigation. Environ. Res. **234**, 116609 (2023)
20. S. Amalraj, R. Murugan, P. Gangapriya, J. Krupa, M. Divya, S.S. Gurav, M. Ayyanar, Evaluation of phytochemicals, enzyme inhibitory, antibacterial and antioxidant effects of *Psydrax dicoccos* Gaertn. Nat. Prod. Res. **36**, 5772–5777 (2022)
21. D. Halarnekar, M. Ayyanar, P. Gangapriya, M. Kalaskar, V. Redasani, N. Gurav, S. Nadaf, S. Saoji, N. Rarokar, S. Gurav, Eco synthesized chitosan/zinc oxide nanocomposites as the next generation of nano-delivery for antibacterial, antioxidant, antidiabetic potential, and chronic wound repair. Int. J. Biol. Macromol. **242**, 124764 (2023)
22. M.S.A. Raj, V. Santhi, S. Amalraj, R. Murugan, P. Gangapriya, V. Pragadheesh, V. Sundaresan, S. Gurav, P. Paramaguru, R. Arulmozhian, A comparative analysis of leaf essential oil profile, in vitro biological properties and in silico studies of four Indian Guava (*Psidium guajava* L.) cultivars, a promising source of functional food. South. Afr. J. Bot. **153**, 357–369 (2023)
23. E.Z. Gomaa, Microbial mediated synthesis of zinc oxide nanoparticles, characterization and multifaceted applications. J. Inorg. Organomet. Polym Mater. **32**, 4114–4132 (2022)
24. J.M. Geyesa, T.B. Esho, B.A. Legesse, A.S. Wotango, Antibacterial and antioxidant potential analysis of *Verbascum sinaiticum* leaf extract and its synthesized silver nanoparticles. Heliyon. **10**(2), e24215 (2024)
25. P.K. Seetharaman, R. Chandrasekaran, S. Gnanasekar, G. Chandrakasan, M. Gupta, D.B. Manikandan, S. Sivaperumal, Antimicrobial and larvicidal activity of eco-friendly silver nanoparticles synthesized from endophytic fungi *Phomopsis Liquidambaris*. Biocatal. Agric. Biotechnol. **16**, 22–30 (2018)
26. A.A. Lekshmi, A. Jayakumar, A. Sunilkumar, A. Shyam, S.S. Chandran, (2024) Synthesis, characterization and versatile applications of silver nanoparticles–A bioinspired approach. Materials Today: Proceedings. https://doi.org/10.1016/j.matpr.2024.01.014
27. M.J. NajeerAhamed, R. Soundharajan, H. Srinivasan, (2023) Antibacterial, antibiofilm, and antivirulence effects of nanoparticles synthesized from *Colletotrichum gloeosporioides* in pathogenic *E. coli*. Microbial Pathogenesis. 185:106420
28. D. Singh, V. Rathod, S. Ninganagouda, J. Herimath, P. Kulkarni, Biosynthesis of silver nanoparticle by endophytic fungi *Penicillium* sp. isolated from *Curcuma longa* (turmeric) and its antibacterial activity against pathogenic gram negative bacteria. J. Pharm. Res. **7**(5), 448–453 (2013)
29. H. Daoudi, A. Bouafia, S. Meneceur, S.E. Laouini, H. Belkhalfa, R. Lebbihi, B. Selmi, Secondary metabolite from *Nigella sativa* seeds mediated synthesis of silver oxide nanoparticles for efficient antioxidant and antibacterial activity. J. Inorg. Organomet. Polym Mater. **32**, 4223–4236 (2022)
30. M.A. Basheer, K. Abutaleb, N.N. Abed, A.A. Mekawey, Mycosynthesis of silver nanoparticles using marine fungi and their antimicrobial activity against pathogenic microorganisms. J. Genetic Eng. Biotechnol. **21**(1), 127 (2023)
31. F. Kurniawan, F.S. Sigit, S. Trompet, E. Yunir, T.J. Tarigan, D.S. Harbuwono, P. Soewondo, D.L. Tahapary, de R. Mutsert, (2024) Lifestyle and clinical risk factors in relation with the prevalence of diabetes in the Indonesian urban and rural populations: the 2018 Indonesian Basic Health Survey. Prev. Med. Rep. 102629
32. K.B. Ishnava, (2024) Biogenic synthesis of silver nanoparticles from the leaf extract of *Enicostema axillare* (poir. Ex Lam.) A. Raynal and its alpha amylase inhibition activity. Food Chem. Adv. 100624

33. M.R. Suchithra, S. Bhuvaneswari, P. Sampathkumar, R. Dineshkumar, K. Chithradevi, R. Madhumitha, M. Kavisri, In vitro study of antioxidant, antidiabetic and antiurolithiatic activity of synthesized silver nanoparticles using stem bark extracts of *Hybanthus Enneaspermus*. Biocatal. Agric. Biotechnol. **38**, 102219 (2021)
34. X. Liu, H. Xu, H. Peng, L. Wan, D. Di, Z. Qin, L. He, J. Lu, S. Wang, Q. Zhao, Advances in antioxidant nanozymes for biomedical applications. Coord. Chem. Rev. **502**, 215610 (2024)
35. M.R. Hasan, M.M. Haque, M.A. Hoque, S. Sultana, M.M. Rahman, M.A. Shaikh, M.K. Sarker, (2024) Antioxidant activity study and GC-MS profiling of *Camellia sinensis* Linn. Heliyon **10**(1)
36. A.S. Yaglioglu, R. Erenler, E.N. Gecer, N. Genc, Biosynthesis of silver nanoparticles using *Astragalus flavesces* leaf: identification, antioxidant activity, and catalytic degradation of methylene blue. J. Inorg. Organomet. Polym Mater. **32**, 3700–3707 (2022)